JOURNAL OF SOLID STATE CHEMISTRY 103, 403–414 (1993)

Homologues of Mo_4O_{11}(mon) in the Mo–W–O System Prepared by Soft Chemistry

F. PORTEMER,* M. SUNDBERG,† L. KIHLBORG,† AND M. FIGLARZ*

Université de Picardie, Laboratoire de Réactivité et de Chimie des Solides, URA CNRS 1211, 33 rue Saint-Leu, F-80039 Amiens Cedex, France; and †Department of Inorganic Chemistry, Arrhenius Laboratory, Stockholm University, S-106 91 Stockholm, Sweden

Received July 1, 1992; accepted September 14, 1992

In specimens prepared by gentle reduction of the mixed oxide $Mo_{0.72}W_{0.28}O_3$ (ReO_3-type structure) phases isotypic of the monoclinic form of Mo_4O_{11} have been observed and characterized by electron diffraction and high resolution electron microscopy techniques. The structures are built up of corner-sharing MO_6 octahedra in ReO_3-type slabs of different widths (m), connected by MO_4 tetrahedra so that alternating four- and six-sided tunnels are formed. The phases are considered as members $m = 7$ and $m = 8$ of a homologous series of structures with the general formula $M_{m+2}O_{3m+4}$, where Mo_4O_{11} is the member $m = 6$. General expressions for the unit cell dimensions are given. Some defects are observed and models are proposed.

Introduction

Mixed oxide phases in the system $Mo_xW_{1-x}O_3$ have been prepared by a conventional high-temperature (500–1100°C) synthesis technique (*1–3*). These phases have a structure of the ReO_3 type, except for the compositions close to MoO_3, where a solid solution of WO_3 in MoO_3 extends to $x \approx 0.95$ (*2, 3*).

More recently, it has been shown that new mixed oxides may be prepared using soft chemistry routes by dehydration of $Mo_xW_{1-x}O_3 \cdot \frac{1}{3} H_2O$ at about 300°C (*4, 5*). For $0 \leq x < 0.6$ a hexagonal structure is obtained, while for $0.6 < x \leq 1$ the structure is related to ReO_3. The new oxides prepared in this way are metastable and transform irreversibly to the thermodynamically stable phases upon heating to around 400°C.

In the reduced system $Mo_xW_{1-x}O_{3-y}$, phases with crystallographic shear (CS) structures, analogous to those found in the binary WO_{3-y} system, have been prepared for low values of y (*6–8*). At slightly higher degrees of reduction, mixed phases isostructural with Mo_5O_{14} and $Mo_{17}O_{47}$ occur (*9*). In addition to MO_6 octahedra they contain "pentagonal columns" (an MO_7 pentagonal bipyramid sharing its five equatorial edges with octahedra). The high-temperature phase relations in the W–Mo–O system have been discussed by Ekström *et al.* (*10*).

In view of the structural differences between the mixed trioxide phases formed by high-temperature and soft chemistry routes, it was considered highly interesting to subject the new trioxide phases to gentle reduction. After soft reduction of a sample of composition $Mo_{0.72}W_{0.28}O_3$, new phases

0022-4596/93 $5.00

were observed which can be considered as members of a new homologous series.

Experimental

The starting material $Mo_{0.72}W_{0.28}O_3$, prepared as described in Ref. (*4*), was reduced at 350°C under H_2 flow for 72 hr, quenched to room temperature, and kept in a glovebox under dry argon until observation. X-ray diffraction patterns were recorded in a Guinier–Lenné camera using Cu$K\alpha$ radiation.

For the electron microscopy investigation a small amount of the specimen (not crushed) was dispersed in *n*-butanol. A drop of the suspension was deposited on a holey carbon film supported on a Cu grid. The grids were then examined in a JEOL JEM 200CX electron microscope, equipped with a top-entry double-tilt lift goniometer stage (max tilt ±10°) and operated at an accelerating voltage of 200 kV. The spherical aberration constant was C_s = 1.2 mm and the radius of the objective aperture used corresponded to 0.41 Å^{-1} in reciprocal space. Simulated image calculations were made based on the multislice method using a locally modified version of the SHRLI suite of programs (*11*).

Results

The reduced sample, $Mo_{0.72}W_{0.28}O_{3-y}$, seemed to be a mixture of several phases. The X-ray powder pattern displayed only very diffuse lines. Some lines could be identified as representing the starting material $Mo_{0.72}W_{0.28}O_3$, while others could not be easily indexed.

The electron diffraction (ED) study confirmed that some fragments were built up of an ordered ReO_3-type structure like that of the starting material. However, some patterns showed weak streaking of the reflections similar to that previously observed for WO_{3-y} CS structures (*12*), suggesting that a slight reduction of the $Mo_{0.72}W_{0.28}O_3$ phase had taken place.

Another type of ED-pattern recorded from several fragments is illustrated in Fig. 1a. From this pattern approximate lattice constants were calculated to be $a \approx 13.9$ Å (true value doubled; see below), $c \approx 6.7$ Å, and $\beta \approx 95°$. Weak streaking of some spots can be distinguished along the [100] direction, and indicates some disorder in the structure along the *a*-axis. Figure 1a also shows that there is a marked substructure in this projection with a rectangular lattice of dimensions 3.8 Å and 2.7 Å. These values are very close to the 100 and 011 spacings observed in the ReO_3-type structure of the starting material and suggest that the crystal is built up of domains based on an ReO_3-type network oriented so that $[110]_c$ (referring to the cubic ReO_3-type subcell) is parallel to the beam. This also gave a reasonable length of the *b*-axis, $b \approx 5.4$ Å.

The HREM image in Fig. 1b shows a well-ordered crystal region, oriented so that the crystal *b*-axis is parallel to the electron beam. The contrast features can be described as slabs, composed of parallel, alternatingly white and black bars. The slabs are mutually linked so that regularly spaced big white dots are formed. A structure model, shown in Fig. 1c, has been derived from the features in the HREM image and the information obtained from the ED pattern. This structure can be described as built up of ReO_3-type slabs cut parallel to $\{211\}_c$ of the basic ReO_3 cell. The slabs are seven MO_6-octahedra wide (m = 7) along $[011]_c$ and linked by MO_4-tetrahedra in such a way that alternating four- and six-sided tunnels are formed. The six-sided tunnels correspond to the large white dots in the HREM image. The stoichiometry of the model in Fig. 1c is M_9O_{25} (Z = 2). The structure is isotypic with that of Mo_4O_{11}(mon) previously reported (*14*). In the Mo_4O_{11}(mon) structure, the width of the ReO_3-type slabs in the $[011]_c$ direction is 6 instead of 7 MO_6-

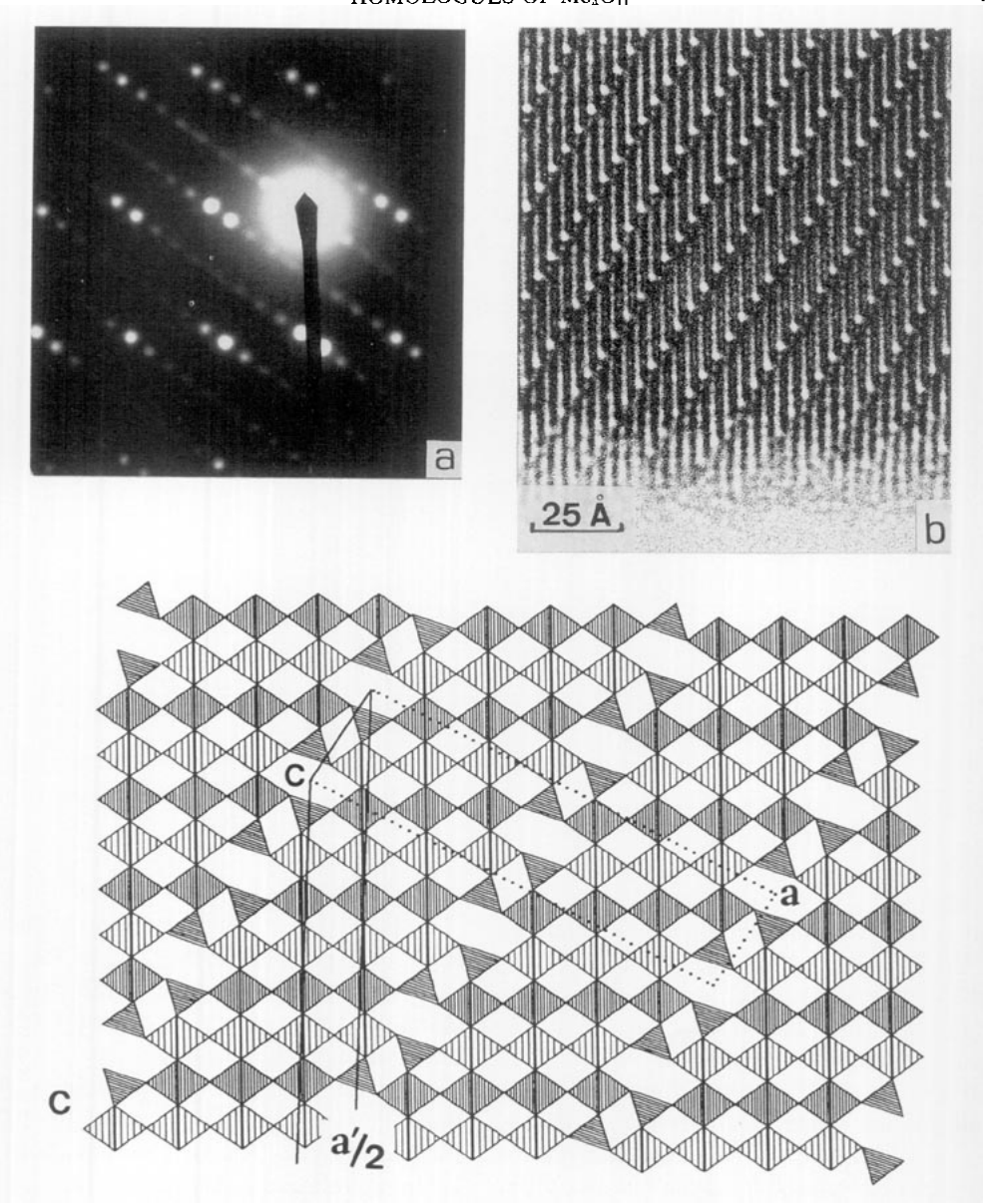

FIG. 1. ED-pattern of $(Mo,W)_9O_{25}$ projected along [010] (a), corresponding HREM image of a well-ordered region (b), idealized structure model of $(Mo,W)_9O_{25}$ ($m = 7$) (c), calculated images at a crystal thickness ≈22 Å (d), HREM image with the calculated image inserted, crystal thickness ≈22 Å, defocus value −700 Å (e).

octahedra as in the present case. The M_9O_{25} structure can thus be considered as a member ($m = 7$) of a homologous series of structures based on the structure of Mo_4O_{11}(mon) for which $m = 6$. This will be further discussed below.

From the structure model in Fig. 1c, approximate atomic parameters were derived

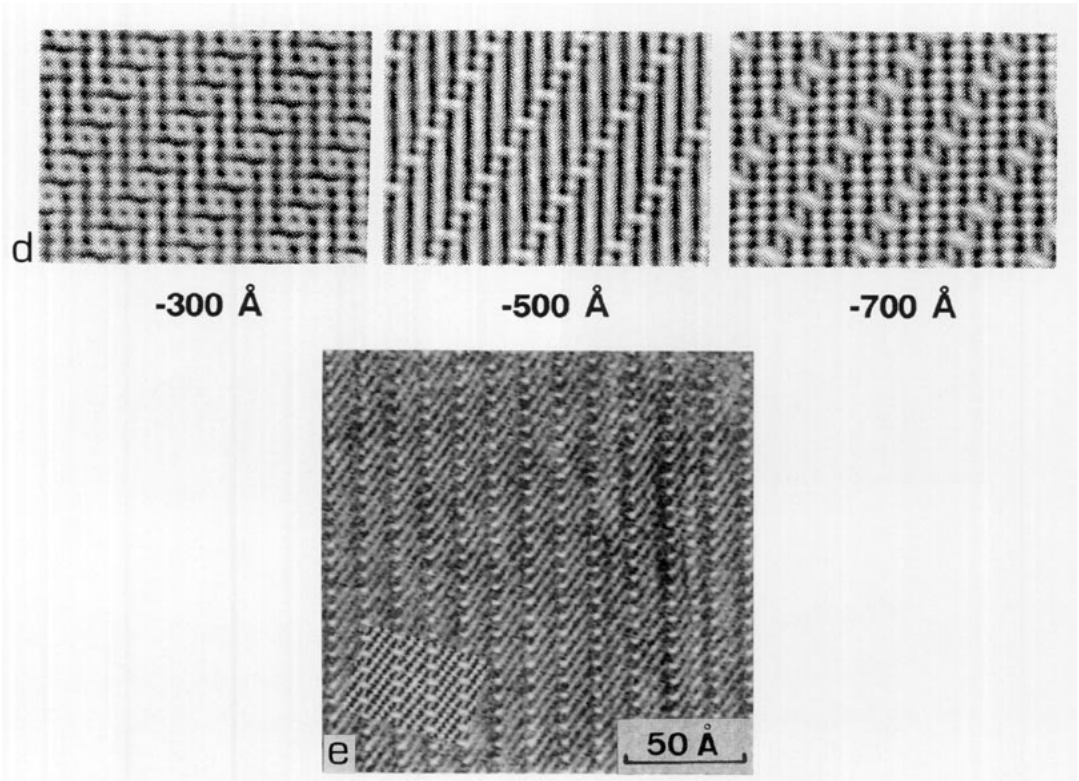

FIG. 1—*Continued*

and used for theoretical image calculations at different crystal thicknesses and defocus values. Some simulated images are shown in Fig. 1d. Fig. 1e illustrates that there is good agreement between the experimental and the inserted simulated image, which confirms the model of the structure.

The ED study showed that there exist some closely related structures, which differ only in the width of the ReO_3-type slabs. This is illustrated by the ED patterns in Fig. 2 which represent two other members (m = 4 and m = 8) of the homologous series based on the Mo_4O_{11}(mon) structure.

Homologues of Mo_4O_{11}(mon)

Mo_4O_{11} has been prepared in two modifications: orthorhombic (*13*) and monoclinic (*14*). Both structures are built up of slabs of ReO_3-type cut parallel to {211} of the cubic subcell. The slabs are 3 octahedra wide along one of the subcell axes and 6 octahedra wide along the two others, and are mutually connected by MoO_4 tetrahedra along the $(211)_c$ planes, corresponding to (100) in the Mo_4O_{11} cell. The two modifications differ in the relative orientation of the slabs: in the monoclinic form all the slabs are in the same orientation (Fig. 4) while in the orthorhombic modification every second slab is reversed (Fig. 3).

The structures obviously give the possibility of homologues having ReO_3-type slabs of different thickness, as noted by Kihlborg (*15*, *16*). The general formula for such homologous series would be $Mo_{m+2}O_{3m+4}$, where m is the number of octahedra along

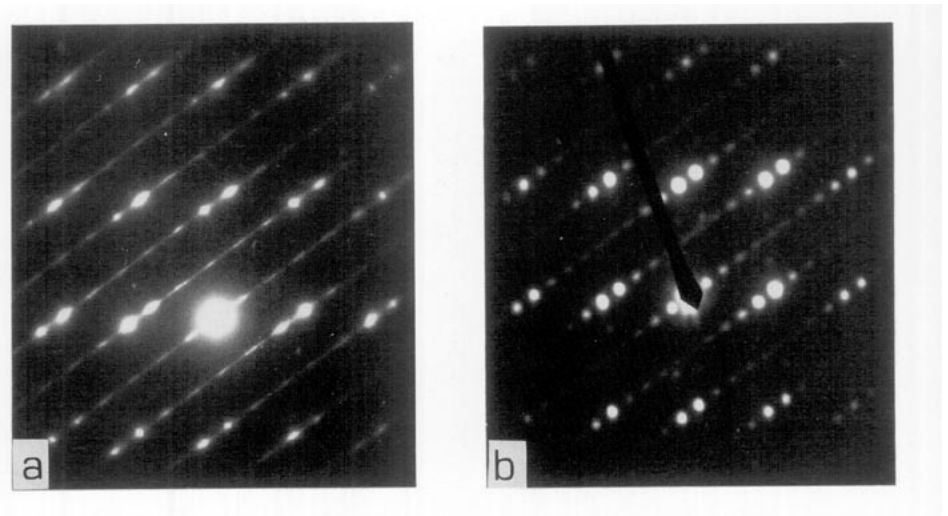

FIG. 2. ED-patterns projected along [010] of two members of the homologous series $M_{m+2}O_{3m+4}$: $m = 4$ (a) and $m = 8$ (b).

$[010]_c$ or $[001]_c$, and $(211)_c$ is the boundary plane of the slab. Mo_4O_{11} is thus the member with $m = 6$, as mentioned above.

The ordered phases, identified by their ED patterns and HREM images in the present study of the mixed molybdenum tungsten system, represent the members of the monoclinic series with $m = 4$, 7, and 8 (see ED patterns in Fig. 1a and Fig. 2).

Structure models can be derived for the different members of the homologous series starting from the known structure of Mo_4O_{11}(mon). The structures are conveniently described in a unit cell where the long axis is approximately parallel to $[011]_c$, as indicated in Fig. 4. The conventional cell of Mo_4O_{11}(mon) should then be changed according to

$$\mathbf{a}' = \mathbf{a} + 6\,\mathbf{c}; \quad \mathbf{b}' = \mathbf{b}; \quad \mathbf{c}' = \mathbf{c}.$$

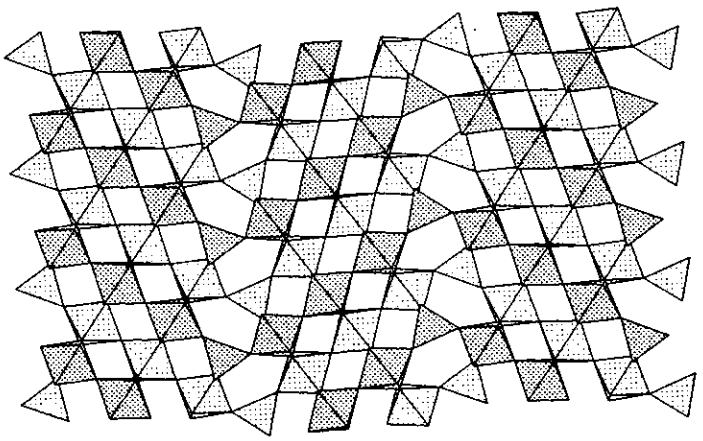

FIG. 3. Structure model of Mo_4O_{11} (o-rh) projected along [010].

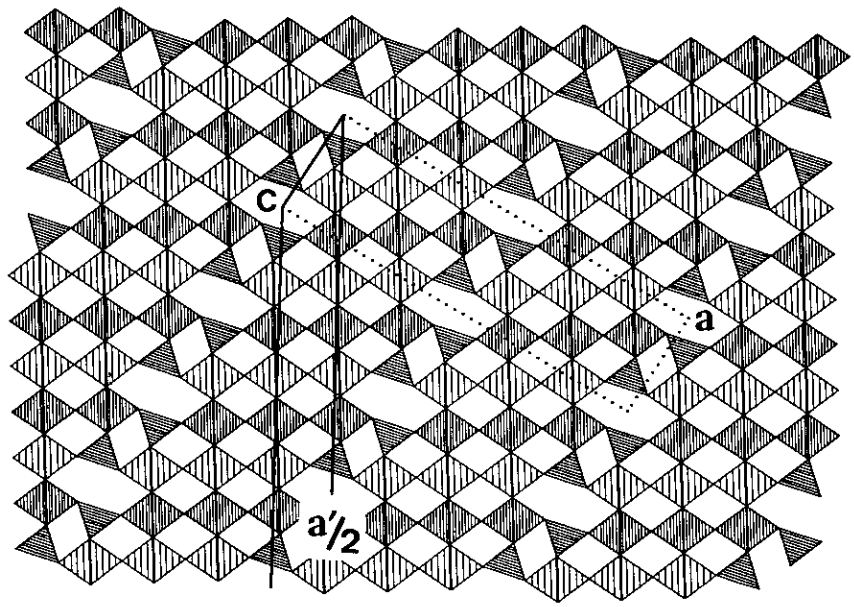

FIG. 4. Idealized structure model of Mo_4O_{11}(mon) ($m = 6$) with the two different cells drawn.

Unit cell dimensions of this new cell are given in Table I together with those of the unit cells calculated for $m = 7$ and $m = 8$. The general expressions for the length of the a axis and the β angle, based on the observed parameters of Mo_4O_{11}(mon), are

$$a' = 45.51 + (m - 6)5.128 \text{ [Å]}$$
$$\beta' = 32.53 + (m - 6)0.11 \text{ [°]}.$$

Only the homologues of the *monoclinic* form of Mo_4O_{11} have been observed in this study, where the samples were prepared at low temperature. This is in accord with the fact that Mo_4O_{11}(mon) is the low-temperature form obtained only below approximately 600°C (*16*). Homologues of the *orthorhombic* form should thus be expected in samples prepared at higher temperatures. Such studies are under way and will be reported in a forthcoming article (*17*).

The structure of Mo_4O_{11}(mon) (*14*) has a unit cell that extends over two ReO_3-type

TABLE IA

UNIT CELL DIMENSIONS FOR Mo_4O_{11}(mon) AND TWO HOMOLOGUES IN ALTERNATIVE CHOICES OF CELLS

m	Formula	a' [Å]	β' [°]	a_r [Å]	β_r [°]
6	Mo_8O_{22}	45.513	32.526	24.540	94.281
7	Mo_9O_{25}	50.64	32.64	27.34	95.23
8	$Mo_{10}O_{28}$	55.77	32.75	30.17	90.00

Note. The values for Mo_4O_{11} are the observed ones [*16*], while the values for the other two structures are estimated. a' and β' refer to the cells with **a** approx. parallel to $[011]_c$, while a_r and β_r refer to the corresponding reduced cells. The two other axes are assumed constant at the values observed for Mo_4O_{11}(mon): $b = 5.439$ Å, $c = 6.701$ Å.

TABLE IB

UNIT CELL DIMENSIONS FOR THREE MONOPHOSPHATE TUNGSTEN BRONZES REPORTED IN THE LITERATURE, WITH THE AXES LABELED TO ALLOW DIRECT COMPARISON WITH THE AXES CALCULATED FOR Mo_4O_{11}(mon) AND ITS HOMOLOGUES (TABLE IA)

m	Formula	a	b	c [Å]	β [°]	Ref.
6	$Na_xP_2W_6O_{22}$	23.775	5.291	6.588	93.47	(*22*)
7	$K_xP_2W_7O_{25}$	27.06	5.3483	6.660	97.20	(*23*)
7	$Na_xP_2W_7O_{25}$	27.076	5.304	6.575	96.17	(*24*)

Note. The last phase is triclinic with α and γ close to 90°.

slabs because corresponding atoms in adjoining slabs are slightly displaced relative to each other parallel to the b-axis. All members with even m will, however, have a marked subcell with $a_s = a/2$. In projection along the b-axis the doubling of the a axis is not observed, however. The odd members, on the other hand, will have a reversal of the height of the tetrahedra at adjacent boundaries so the doubling of the a axis will be more pronounced in this case, although, again, it will not be visible in the projection along the b axis. The space group will be $P2_1/a$ (as for Mo_4O_{11}) for even members, and $P2/a$ for odd ones.

Atomic coordinates can be estimated for the members with $m = 7$ and $m = 8$ based on the known structure of Mo_4O_{11}(mon). These are given in Table II. They give reasonable interatomic distances, but how closely they apply to the Mo–W oxides under discussion here is not known. These parameters have been used to calculate simulated HREM images.

Defects and Disorder

The streaking of the reflections along [100] (see Fig. 1a) indicates that the width of the ReO_3-type slabs varies. Figure 5 illustrates a different region of the same fragment as in Fig. 1b, where both wider and narrower ReO_3-type slabs can be seen.

Another type of defect sometimes observed in the HREM images is shown in Fig. 6a. Thin slabs of MO_4-tetrahedra (M = Mo, W) are shifted laterally at the arrows. An interpretation consistent with the image (Fig. 6b) shows that the width of the ReO_3-type slabs changes by one MO_6-octahedron at these faults. This kind of defect alters slightly the width of the ReO_3-type slabs and might suggest an ordering mechanism following the initial formation of a more or less disordered crystal.

Many of the crystals examined by HREM appeared not to be completely stable in the electron microscope. A slight reduction of the crystal fragments seemed to take place when they were subjected to the electron beam and high vacuum in the microscope. Similar observations have previously been reported for slightly reduced tungsten trioxide crystals where formation and growth of new CS-planes under the influence of the electron beam in the microscope have been observed (*18*). Figure 7a shows the HREM image of a fairly well-ordered thin crystal fragment, where the width of the ReO_3-type slabs mainly corresponds to the members $m = 7$ and $m = 8$ of the homologous series based on the monoclinic Mo_4O_{11}-type structure. Figure 7b shows the micrograph of the same crystal region after exposure to the electron beam for several minutes. This HREM image clearly suggests that new planes composed of MO_4-tetrahedra have been formed both from the crystal edge and

TABLE II

STRUCTURE MODELS FOR THE TWO HOMOLOGUES OF Mo_4O_{11}(mon) ($m = 6$) WITH $m = 7$ AND $m = 8$

	Homologue $m = 7$, $a = 50.64$ Å, $b = 5.439$ Å, $c = 6.701$ Å, $\beta = 32.64°$ Space group: $P2/a$			Homologue $m = 8$, $a = 55.77$ Å, $b = 5.439$ Å, $c = 6.701$ Å, $\beta = 32.75°$ Space group: $P2_1/a$		
	x	y	z	x	y	z
M	.03887	.21434	.05447	.03530	.21434	.05447
	.09139	.73691	.04705	.08281	.73691	.04871
	.14659	.22622	.01730	.13220	.22622	.02615
	.19854	.72936	.00888	.17924	.72936	.01939
	.25000	.2300	.00000	.22632	.2300	.00775
O	.0226	.7447	.6305	.0205	.7447	.6305
	.0554	.4412	.1236	.0502	.4412	.1244
	.0466	.9228	.1148	.0423	.9228	.1156
	.0787	.2324	.5974	.0708	.2324	.6044
	.1149	.5164	.0603	.1038	.5164	.0656
	.1079	.0121	.0662	.0974	.0121	.0715
	.1383	.7290	.5696	.1236	.7290	.5896
	.1707	.4501	.0336	.1540	.4501	.0433
	.1638	.9590	.0429	.1477	.9590	.0526
	.1964	.2292	.5212	.1773	.2292	.5312
	.2236	.9966	.9924	.2000	.9950	.0220
	.2258	.4966	.0076	.2023	.4950	.0340
	.2500	.7300	.5000	.2258	.7300	.5100
				.2520	.0000	.9594

Note. The unit cell dimensions and atomic coordinates have been derived by introducing one and two additional octahedra, respectively, into the rows of the ReO_3-type slabs.

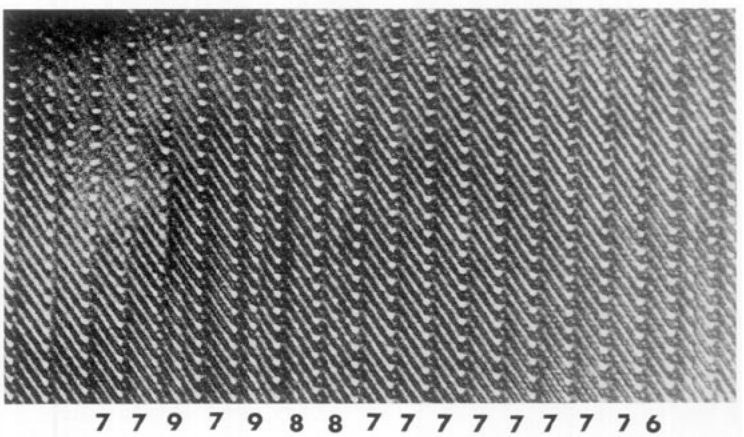

FIG. 5. HREM image of a disordered fragment $\approx M_9O_{25}$. The variation in width (m) is indicated.

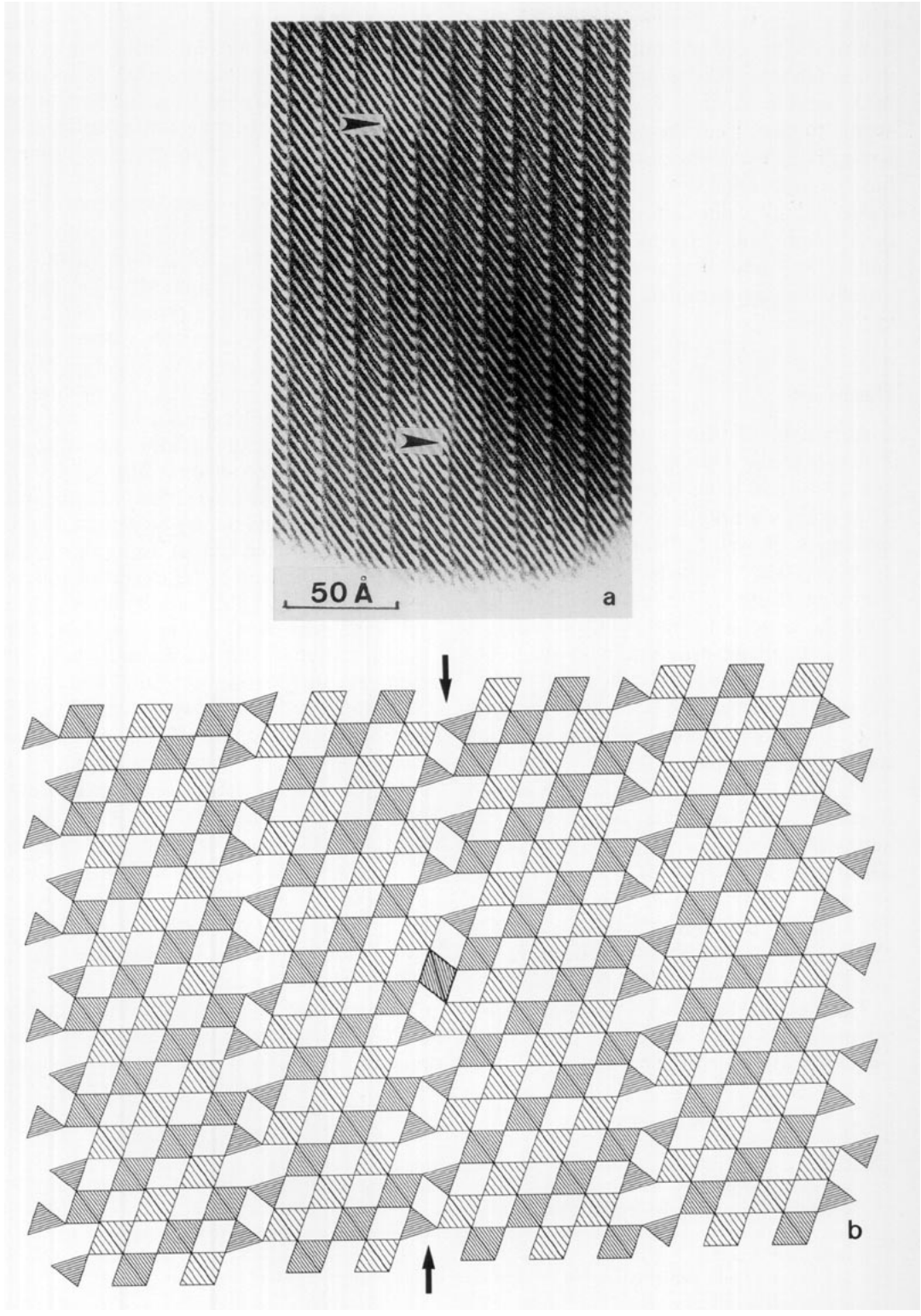

FIG. 6. HREM image illustrating some defects marked by arrows (a). An interpretation of the defect is shown in the idealized structure model (b).

inside the crystal. This means that a reduction of the crystal has taken place. The reduction involves oxygen loss, transforming MO_6 octahedra into MO_4 tetrahedra. It seems to start from the crystal surface. At some places it can be seen that the reduction has not proceeded through the crystal. The model in Fig. 7c illustrates a slab (with initial $m = 7$) split into two new slabs with $m = 2$ and $m = 3$ and also how a slab of MO_4-tetrahedra can terminate inside the ReO_3-type network.

Discussion

Although all efforts to prepare homologues of the two Mo_4O_{11} forms in the binary Mo–O system have been futile so far, Raveau and co-workers have found such homologues in reduced tungsten phosphate systems. The so called *monophosphate tungsten bronzes*, designated "$MPTB_P$," with the general formula $(PO_2)_2(WO_3)_m$, $2 \leq m \leq 10$, are isostructural with Mo_4O_{11} (o-rh) (*19, 20*). A series, called "$MPTB_H$," based on the structure of Mo_4O_{11}(mon) can also be prepared if alkali is introduced into the hexagonal tunnels: $A_x(PO_2)_2(WO_3)_m$ (A = Na or K) (*21*). Members with m ranging from 4 to 13 have been observed in this series (*20*), and the crystal structures of the members with $m = 4$ (*21, 22*), $m = 6$ (*22*), and $m = 7$ (*23, 24*) have been determined. Phosphate niobium bronzes $A_x(PO_2)_2(NbO_3)_m$ of the "$MPTB_P$" type have also been prepared recently (*25, 26*).

The mixed Mo–W oxides reported here are obviously of the same structural type as the "$MPTB_H$" series. There is no evidence for any alkali atoms occupying the hexagonal tunnels in the present phases, however, nor is any alkali present during the synthesis. As seen in Table I the agreement between the unit cell dimensions is rather good despite the difference in chemical composition.

The question why homologues of the two Mo_4O_{11} forms can be prepared only with tungsten substituting for part of the molybdenum and not in the pure Mo–O system is an interesting one. It is probably related to the distortion pattern and the valency distribution within the ReO_3-type slabs (*27*). A further question related to this problem is whether the molybdenum and tungsten atoms are statistically distributed or if segregation to the tetrahedra and across the ReO_3-type slabs occurs. If such segregation is present, it could hardly be detected in the HREM images and further discussion of this problem must await better experimental evidence from X-ray diffraction studies.

In the Mo–W–O ternary system containing molybdenum as a major metallic element, the dominating structural mechanism for a slight reduction down to $O/M \approx 2.87$ is crystallographic shear (CS). CS structures based on MoO_3 have been observed in tungsten-free samples (*27*), while CS in an ReO_3-type lattice occurs in the M_nO_{3n-1} series with $n = 8$–14, where partial substitution by tungsten is required to form phases with $n > 9$ (*6*). The ReO_3-type elements in this latter series form slabs which are infinite in two dimensions and joined by edge sharing along the shear planes.

At higher degrees of reduction and moderately high temperatures (500–700°C) two phases containing pentagonal columns

FIG. 7. Micrographs of a thin crystal fragment taken (a) after short exposure to the beam and (b) after exposure to the beam for several minutes. New reduction planes are indicated by arrows. (c) Idealized structure model showing a reduction plane introduced in the lower part (arrowed) and terminating inside the structure. The obvious strains of the polyhedra around the defect in this model and that of Fig. 6 can be substantially reduced by relaxation within a larger region of the lattice.

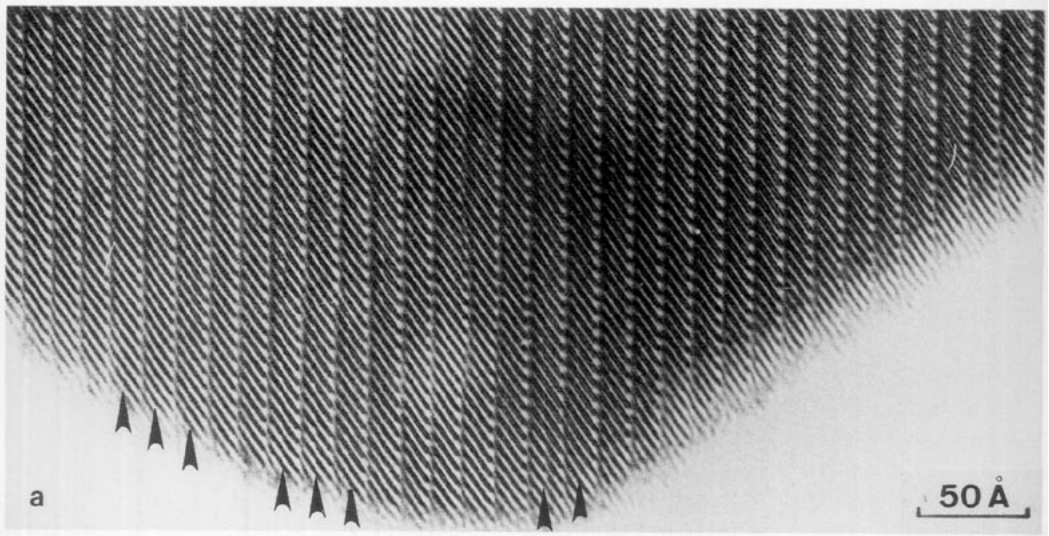
a
50 Å

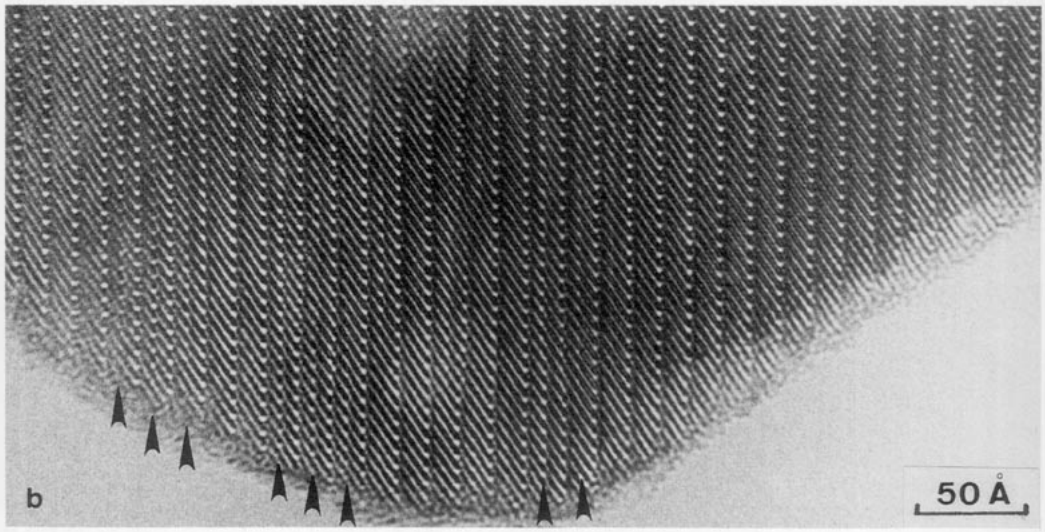
b
50 Å

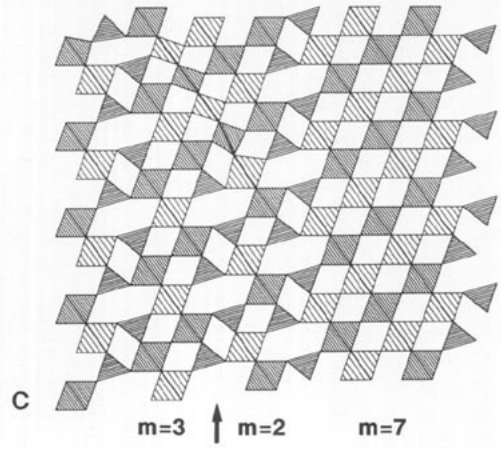
C
m=3
m=2
m=7

(PCs) form, viz. M_5O_{14} and $M_{17}O_{47}$ at $O/M = 2.80$ and 2.77, respectively. Both phases can contain appreciable amounts of tungsten (*9, 10*). Although these rather complex structures can be derived formally from an ReO_3-type basic structure (*28–30*), there is no simple relation. Two-dimensionally infinite ReO_3-type blocks reoccur in the Mo_4O_{11} structures at only slightly higher reduction, $O/M = 2.75$, but now separated by tetrahedra.

The present homologues of Mo_4O_{11} have O/M ratios in the range where the PC phases are stable, at least at higher temperatures. The decomposition of the present phases at low temperature does not yield PC phases, however, but CS phases containing ReO_3-type slabs. The formation of the present homologues is thus very likely governed by kinetic constraints at the low reaction temperature used in the soft chemistry synthesis.

Further studies of these phases are being made, aiming among other things at an understanding of the relation between the W/Mo ratio and the structures formed.

Acknowledgment

We thank Carole Génin (Amiens) for preparing the specimens and Jaroslava Östberg (Stockholm) for technical assistence with photographic work. F. P. thanks the Centre National de la Recherche Scientifique for financial support which made his stay at the Arrhenius Laboratory possible. This study has been supported by the Swedish Natural Science Research Council.

References

1. A. Magnéli, *Acta Chem. Scand.* **3,** 88 (1949).
2. S. Westman and A. Magnéli, *Acta Chem. Scand.* **12,** 363 (1958).
3. E. Salje, R.Gehlig, and K. Wiswanathan, *J. Solid State Chem.* **25,** 239 (1978).
4. F. Harb, B. Gerand, and M. Figlarz, *C.R. Acad. Sci. Paris Ser. II* **303,** 789 (1986).
5. F. Harb, B. Gerand, and M. Figlarz, *C.R. Acad. Sci. Paris Ser. II* **303,** 445 (1986).
6. A. Magnéli, B. Blomberg-Hansson, L. Kihlborg, and G. Sundkvist, *Acta Chem. Scand.* **9,** 1382 (1955).
7. L. A. Bursill and B. G. Hyde, *J. Solid State Chem.* **4,** 430 (1972).
8. K. Viswanathan and E. Salje, *Acta Crystallogr. Sect. A,* **37,** 449 (1981).
9. T. Ekström, *Mater. Res. Bull.* **7,** 19 (1972).
10. T. Ekström, E. Salje, and R. J. D. Tilley, *J. Solid State Chem.* **40,** 75 (1981).
11. M. A. O'Keefe, P. R. Buseck, and S. Iijima, *Nature (London)* **274,** 322 (1978).
12. M. Sundberg, *Chem. Commun. Univ. Stockholm,* **No. 5** (1981).
13. A. Magnéli, *Acta Chem. Scand.* **2,** 861 (1948).
14. L. Kihlborg, *Arkiv Kemi* **21,** 365 (1963).
15. L. Kihlborg, *Adv. Chem. Ser.* **39,** 37 (1963).
16. L. Kihlborg, *Acta Chem. Scand.* **13,** 954 (1959).
17. M. Sundberg, B.-O. Marinder, and F. Portemer, to be published.
18. M. Sundberg and R. J. D. Tilley, *Phys. Status Solidi A* **22,** 677 (1974).
19. J. P. Giroult, M. Goreaud, A. Grandin, P. Labbé, and B. Raveau, *Acta Crystallogr. Sect. B* **37,** 2139 (1981).
20. M. M. Borel, M. Goreaud, A. Grandin, P. Labbé, A. Leclaire, and B. Raveau, *Eur. J. Solid State Inorg. Chem.* **28,** 93 (1991).
21. J. P. Giroult, M. Goreaud, P. Labbé, and B. Raveau, *J. Solid State Chem.* **44,** 407 (1982).
22. A. Benmoussa, D. Groult, P. Labbé, and B. Raveau, *Acta Crystallogr. Sect. C* **40,** 573 (1984).
23. B. Domengès, M. Goreaud, P. Labbé, and B. Raveau, *J. Solid State Chem.* **50,** 173 (1983).
24. M. Lamire, P. Labbé, M. Goreaud, and B. Raveau, *J. Solid State Chem.* **66,** 64 (1987).
25. A. Benabbas, M. M. Borel, A. Grandin, A. Leclaire, and B. Raveau, *J. Solid State Chem.* **95,** 245 (1991).
26. G. Costentin, M. M. Borel, A. Grandin, A. Leclaire, and B. Raveau, *Mater. Res. Bull.* **26,** 1051 (1991).
27. L. Kihlborg, *Arkiv Kemi* **21,** 471 (1963).
28. B. G. Hyde and M. O'Keeffe, *Acta Crystallogr. Sect. A* **29,** 243 (1973).
29. B. G. Hyde, A. N. Bagshaw, S. Andersson, and M. O'Keeffe, *Ann. Rev. Mater. Sci.* **4,** 43 (1974).
30. B.-O. Marinder, *Angew Chem.* **5,** 430 (1986).